Contemporary Mathematics
https://ojs.wiserpub.com/index.php/CM/

Research Article

On Solving Caputo Fractional Windkessel Model with System of Cardiovascular Circulatory by Using Some Residual Maps Technique

Faten H. Damag[1*], **Amin Saif**[2]

[1]Department of Mathematics, Faculty of Sciences, Hail University, Hail, 2440, Saudi Arabia
[2]Department of Mathematics, Faculty of Applied Sciences, Taiz University, Taiz, Yemen
E-mail: fat.qaaed@uoh.edu.sa

Received: 15 September 2025; **Revised:** 21 October 2025; **Accepted:** 23 October 2025

Abstract: The Windkessel model provides a simplified framework for representing the cardiovascular system, emphasizing the role of arterial elasticity. It elucidates how the compliance of major arteries smooths the heart's pulsatile pumping, resulting in a steadier blood flow. This work utilizes the Caputo fractional operator to derive analytical solutions for the Windkessel model within standard topological Banach spaces. We introduce a novel approach called the Sawi Residual Power Series Technique (SRPST), which combines the Sawi transform with the residual power series method. This technique allows for a thorough investigation of the modified Caputo fractional Windkessel model. Our studies demonstrate the efficiency, reliability, and capability of SRPST in deriving analytical solutions, supported by various numerical and graphical analyses. The results not only validate the proposed method but also highlight its potential applications in broader fields such as fluid dynamics and biomedical engineering.

***Keywords*:** residual power series, Caputo derivative operator, Sawi transform

MSC: 34A34, 35A20, 44A10

1. Introduction

The theory of differential equations is regarded as one of the most important subjects in the broad field of sciences, with extensive applications in physics, mathematics, medicine, wave theory, and fluid dynamics. In recent years, growing attention has been directed toward fractional calculus, which has emerged as both a practical tool and a dynamic branch of modern mathematics. Fractional calculus extends classical integer-order equations to their fractional counterparts, allowing the formulation and solution of a wide range of problems, thereby giving rise to fractional differential equations. This generalization provides a new mathematical framework that captures complex physical and biological processes more accurately [1–6].

Extensive research has demonstrated the wide applicability of fractional differential equations in diverse fields, including fluid mechanics, electrical networks, groundwater modeling, physics, engineering, and medicine, as well as other branches of science. Several definitions of fractional derivatives have been introduced, among which the Riemann-Liouville fractional differential operator remains the most classical and widely studied. Building on this operator,

DOI: https://doi.org/10.37256/cm.6620258640

researchers have developed other important forms of fractional derivatives, such as the Hilfer derivative, the Caputo derivative, and the Hilfer-Katugampola derivative.

On the integral side, the Riemann-Liouville fractional integral operator is one of the earliest and most fundamental constructions. Over time, many other fractional integral operators have been introduced that extend its foundational concept, including the Hadamard fractional integral operator and the Katugampola fractional integral operator. Further details on fractional integral-differntial operators and their generalizations can be found in [7–10].

One application of differential equations and fractional differential equations is the Windkessel model, which is crucial for representing the dynamic behavior of arteries in the cardiovascular circulatory system. This model aids in understanding the dynamics of blood circulation and the effects of various physiological parameters on blood pressure and flow. It conceptualizes the arterial system as a compliant reservoir that absorbs the pulsatile output of the heart and maintains a steady flow of blood during diastole. The Windkessel model describes the relationship between blood flow and pressure in the cardiovascular system through the following differential equation [11]:

$$C\frac{d\omega(\tau)}{d\tau}+\frac{1}{\sigma}\omega(\tau)=\varphi(\tau)\quad 0<\nu\leq 1, \tag{1}$$

where C is the total compliance of the arterial system, $\varphi(\tau)$ is the rate of blood flow at time τ, $\omega(\tau)$ is the pressure of arteries at time τ and σ is the total vascular resistance.

To provide analysis and analytical solutions for the Windkessel model, several studies have been conducted. For example, Kind et al. [12] employed a non-iterative identification algorithm that utilized physical foreknowledge to estimate parameters in both the three-element and four-element Windkessel models. Fernandes et al. [13] pioneered a novel approach that combines physiologically accurate models with a five-element Windkessel model to enhance the accuracy of hemodynamics and the fractional flow reserve parameter. Gnudi [14] derived time-domain analytical solutions for two-, three-, and four-element Windkessel models, obtaining closed-form expressions for the arterial system. Westerhof et al. [15] introduced characteristic impedance as a third element of the Windkessel model to estimate total arterial compliance based on blood flow and pressure. Gil et al. [16] presented results and analysis related to a two-element Windkessel model, focusing on compliance and vascular resistance within the arterial system. Choudhury et al. [17] utilized the two-element Windkessel model to estimate total peripheral resistance and arterial compliance in individuals, employing various features. Additionally, several studies have introduced analytical solutions and analyses of Windkessel models using fractional operators. Resmi and Selvaganesani [18] introduced fractionality into the existing 2-element, 3-element, and 4-element Windkessel systems. Bahloul and Taous [19] demonstrated that the fractional-order Windkessel model better with analytical s the phase angle. Gamilov and Ruslan [20] proposed combining a one-dimensional model of coronary blood flow in fractional Windkessel conditions, while Traver et al. [21] illustrated the effectiveness of fractional-order behavior in the classic Windkessel model.

We mean by the usual topological Banach space [22], is a family of a Banach $\mathscr{B}$ on $\mathbb{F}$ as afield and $||\cdot||$ as a norm on $\mathscr{B}$ with mertizable topology induced by $||.||$.

Let $\omega(\tau):(0,\infty)\to\mathscr{B}$ be any map on $\mathbb{J}:=(0,\infty)$.

The motivation for this study is to enhance the understanding of the cardiovascular system through the Windkessel model, utilizing fractional calculus to capture complex behaviors in blood flow and pressure. By introducing the Sawi Residual Power Series Technique (SRPST), the study aims to provide innovative solutions to fractional differential equations, demonstrating its efficiency through numerical simulations and graphical analyses. This work not only contributes to cardiovascular modeling but also holds potential applications in various fields like fluid dynamics and medical physics, encouraging interdisciplinary research.

This work employs a technique SRPST to get some analytical solutions of the following fractional differential equation in $\mathscr{B}=\mathbb{R}$

$$C\,{}^{c}\mathscr{D}^{\nu}\omega(\tau)+\frac{1}{\sigma}\omega(\tau)=\varphi(\tau), \tag{2}$$

where ${}^{c}\mathscr{D}^{\nu}$ is the Caputo fractional derivative of order ν. Section 2 recalls the basic concepts and facts related to the Sawi transform and Caputo fractional differential operators. We prove several relevant facts concerning these operators in standard topological Banach space. Section 3 introduces the basic preliminaries and methodology of SRPST.

In section 4, we investigate and present analytical solutions to the fractional differential Equation (2), which represents the Windkessel model for the cardiovascular circulatory system, in the usual topological Banach space $\mathscr{B}=\mathbb{R}$.

In section 5, we provide numerical and graphical analyses of our analytical solutions for the Windkessel model, demonstrating the efficiency, reliability, and capability of the SRPST in finding these solutions.

Finally, section 6 includes discussions and conclusions drawn from our findings.

2. On Caputo operator with Sawi transform

Consider ω is any map on $\mathbb{J}$. The Riemann-Liouville Fractional (R-LF) derivative [23], for $\omega(\tau)$ of order $\nu>0$ is given by

$$\mathscr{D}^{\nu}\omega(\tau)=\mathscr{D}^{m}\mathscr{I}^{\nu}\omega(\tau)\quad m-1<\nu<m, \tag{3}$$

where $m\in\mathbb{N}$ and $\mathscr{I}^{\nu}$ is the R-LF integral [23], for $\omega(\tau)$ of order ν is given by

$$\mathscr{I}^{\nu}\omega(\tau)=\begin{cases}\dfrac{1}{\Gamma(\nu)}\int_0^{\tau}(\tau-\gamma)^{\nu-1}\omega(\gamma)d\gamma, & \nu>0\\ \omega(\tau), & \nu=0.\end{cases} \tag{4}$$

The CFD operator [24, 25], for $\omega(\tau)$ of order ν is given by

$${}^{c}\mathscr{D}^{\nu}\omega(\tau)=\begin{cases}\mathscr{I}^{m-\nu}\left[\dfrac{d^{m}\omega(\tau)}{d\tau^{m}}\right], & m-1<\nu<m\\ \dfrac{d^{\nu}\omega(\tau)}{d\tau^{\nu}}, & \nu\in\mathbb{N}.\end{cases} \tag{5}$$

Recall [24] that for $\tau\geq 0$ and for $m-1<\nu<m$ we have ${}^{c}\mathscr{D}^{\nu}\mathscr{I}^{\nu}\omega(\tau)=\omega(\tau)$ and ${}^{c}\mathscr{D}^{\nu}\tau^{\gamma}=\dfrac{\Gamma(\nu+1)}{\Gamma(\gamma-\nu+1)}\tau^{\gamma-\nu}$.

Let $\omega(\tau)$ be a map with order-exponentiation ρ on $\mathbb{J}$. The Sawi transform $\mathscr{S}_{\theta}$ [26], of $\omega(\tau)$ is defined by

$$\omega^{s}(\theta):=\mathscr{S}_{\theta}\omega(\tau)=\frac{1}{\theta^{2}}\int_0^{\infty}e^{-\frac{\tau}{\theta}}\omega(\tau)d\tau\quad\rho_1\leq\theta\leq\rho_2. \tag{6}$$

The inverse Sawi transform $\mathscr{S}_{\theta}^{-1}$ of $\omega^{s}(\theta)$ is given by

$$\mathscr{S}_{\theta}^{-1}\omega^{s}(\theta)=\omega(\tau). \tag{7}$$

We observe that the Sawi transform and its inverse have linearly properties, that is,
1. $\mathscr{S}_\theta[c_1\omega(\tau)+c_2\varepsilon(\tau)] = c_1\mathscr{S}_\theta\omega(\tau)+c_2\mathscr{S}_\theta\varepsilon(\tau)$, where c_1 and c_2 are constants;
2. $\mathscr{S}_\theta^{-1}[c_1\mathscr{S}_\theta\omega(\tau)+c_2\mathscr{S}_\theta\varepsilon(\tau)] = c_1\omega(\tau)+c_2\varepsilon(\tau)$, where c_1 and c_2 are constants.
Also we have

$$\mathscr{S}_\theta\left[\omega(\tau)*\varepsilon(\tau)\right] = \theta^2\omega^s(\theta)\varepsilon^s(\theta), \tag{8}$$

where

$$\omega(\tau)*\varepsilon(\tau) = \int_0^\tau \omega(\mu)*\varepsilon(\tau-\mu)d\mu.$$

Theorem 1 [1] Let $\omega:\mathbb{J}\to\mathbb{R}$ be any map on $\mathbb{J}$. Then

$$\mathscr{S}_\theta\left[\mathscr{D}^m\omega(\tau)\right] = \theta^{-m}\omega^s(\theta) - \sum_{j=0}^{m-1}\theta^{j-m-1}\mathscr{D}^j\omega(\tau)\Big|_{\tau=0}. \tag{9}$$

Lemma 1 Let $\omega:\mathbb{J}\to\mathbb{R}$ be any map on $\mathbb{J}$. Then
1. $\mathscr{S}_\theta\mathscr{I}^\nu\omega(\tau) = \theta^\nu\omega^s(\theta)$;
2. $\mathscr{S}_\theta\left[{}^c\mathscr{D}^\nu\omega(\tau)\right] = \theta^{-\nu}\omega^s(\theta) - \sum_{j=0}^{n-1}\theta^{j-\nu-1}\mathscr{D}^j\omega(\tau)\Big|_{\tau=0} \quad (n-1<\nu<n)$.

Proof. (1) By the formula of R-L integral, we have

$$\mathscr{I}^\nu\omega(\tau) = \begin{cases} \frac{1}{\Gamma(\nu)}\int_0^\tau(\tau-\gamma)^{\nu-1}\omega(\gamma)d\gamma, & \nu>0 \\ \omega(\tau), & \nu=0. \end{cases} \tag{10}$$

If $\nu=0$ then the proof is clear. If $\nu\neq 0$ then we have

$$\mathscr{I}^\nu\omega(\tau) = \frac{1}{\Gamma(\nu)}\int_0^\tau(\tau-\gamma)^{\nu-1}\omega(\gamma)d\gamma = \frac{1}{\Gamma(\nu)}\left[\tau^{\nu-1}*\omega(\tau)\right]. \tag{11}$$

Take the Sawi transform of the equation above and by Eq. (8),

$$\mathscr{S}_\theta\mathscr{I}^\nu\omega(\tau) = \mathscr{S}_\theta\left[\frac{1}{\Gamma(\nu)}\left[\tau^{\nu-1}*\omega(\tau)\right]\right] = \theta^2\frac{1}{\Gamma(\nu)}\Gamma(\nu)\theta^{\nu-2}\omega^s(\theta) = \theta^\nu\omega^s(\theta).$$

(2) By the formula of Caputo fractional operator, we have

$${}^c\mathscr{D}^\nu\omega(\tau) = \begin{cases} \mathscr{I}^{n-\nu}\mathscr{D}^n\omega(\tau), & n-1<\nu<n \\ \mathscr{D}^\nu\omega(\tau), & \nu\in\mathbb{N}. \end{cases} \tag{12}$$

If $\nu \in \mathbb{N}$ then the proof is trivial from Theorem 1. If $n-1 < \nu < n$ then we have

$$\begin{aligned} {}^{c}\mathscr{D}^{\nu}\omega(\tau) &= \mathscr{I}^{n-\nu}\mathscr{D}^{n}\omega(\tau) = \frac{1}{\Gamma(n-\nu)}\int_0^{\tau}(\tau-\gamma)^{n-\nu-1}\mathscr{D}^{n}\omega(\gamma)d\gamma \\ &= \frac{1}{\Gamma(n-\nu)}\left[\tau^{n-\nu-1} * \mathscr{D}^{n}\omega(\tau)\right]. \end{aligned} \tag{13}$$

Take the Sawi transform of the equation above and use Eq. (8) and Theorem 1 to get

$$\begin{aligned} \mathscr{S}_{\theta}\left[{}^{c}\mathscr{D}^{\nu}\omega(\tau)\right] &= \mathscr{S}_{\theta}\left[\frac{1}{\Gamma(n-\nu)}\left[\tau^{n-\nu-1} * \mathscr{D}^{n}\omega(\tau)\right]\right] \\ &= \frac{\theta^2}{\Gamma(n-\nu)}\Gamma(n-\nu)\theta^{n-\nu-2} * \mathscr{S}_{\theta}\left[\mathscr{D}^{n}\omega(\tau)\right] \\ &= \theta^{n-\nu}\left[\theta^{-n}\omega^{s}(\theta) - \sum_{j=0}^{n-1}\theta^{j-n-1}\mathscr{D}^{j}\omega(\tau)\Big|_{\tau=0}\right] \\ &= \theta^{-\nu}\omega^{s}(\theta) - \sum_{j=0}^{n-1}\theta^{j-\nu-1}\mathscr{D}^{j}\omega(\tau)\Big|_{\tau=0}. \end{aligned} \tag{14}$$

□

Lemma 2 Let $\omega : \mathbb{J} \to \mathbb{R}$ be a map on $\mathbb{J}$. Then

$$\mathscr{S}_{\theta}\left[{}^{c}\mathscr{D}^{k\nu}\omega(\tau)\right] = \theta^{-k\nu}\omega^{s}(\theta) - \sum_{j=0}^{k-1}\theta^{(j-k)\nu-1}\,{}^{c}\mathscr{D}^{j\nu}\omega(\tau)\Big|_{\tau=0} (0 < \nu \leq 1). \tag{15}$$

Proof. We will prove (15) by using the mathematical induction. At $k = 1$, since $0 < \nu \leq 1$ in (15), that is, $n = 0$ in the part (2) of Lemma above. Hence

$$\mathscr{S}_{\theta}\left[{}^{c}\mathscr{D}^{\nu}\omega(\tau)\right] = \theta^{-\nu}\omega^{s}(\theta) - \theta^{-\nu-1}\omega(0). \tag{16}$$

That is, (15) holds at $k = 1$. At $k = 2$, let $\varepsilon(\tau) = {}^{c}\mathscr{D}^{\nu}\omega(\tau)$. By (16) above we have

$$\begin{aligned} \mathscr{S}_{\theta}\left[{}^{c}\mathscr{D}^{\nu}\varepsilon(\tau)\right] &= \theta^{-\nu}\varepsilon^{s}(\theta) - \theta^{-\nu-1}\varepsilon(0) \\ &= \theta^{-\nu}\mathscr{S}_{\theta}\,{}^{c}\mathscr{D}^{\nu}\omega(\tau) - \theta^{-\nu-1}\,{}^{c}\mathscr{D}^{\nu}\omega(\tau)\Big|_{\tau=0} \\ &= \theta^{-\nu}\left[\theta^{-\nu}\omega^{s}(\theta) - \theta^{-\nu-1}\omega(0)\right] - \theta^{-\nu-1}\,{}^{c}\mathscr{D}^{\nu}\omega(\tau)\Big|_{\tau=0} \end{aligned}$$

$$= \theta^{-2\nu}\omega^s(\theta) - \theta^{-2\nu-1}\omega(0) - \theta^{-\nu-1}\,{}^c\mathscr{D}^{\nu}\omega(\tau)\Big|_{\tau=0}. \tag{17}$$

That is, (15) holds at $k=2$. Let (15) is true at $k=m$, that is,

$$\mathscr{S}_\theta\left[{}^c\mathscr{D}^{-m\nu}\omega(\tau)\right] = \theta^{-m\nu}\omega^s(\theta) - \sum_{j=0}^{m-1}\theta^{(j-m)\nu-1}\,{}^c\mathscr{D}^{j\nu}\omega(\tau)\Big|_{\tau=0}. \tag{18}$$

We will prove (15) holds at $k=m+1$. Let $\varepsilon(\tau) = {}^c\mathscr{D}^{m\nu}\omega(\tau)$. By (16) and (18) we have

$$\begin{aligned}
\mathscr{S}_\theta\left[{}^c\mathscr{D}^{k\nu}\varepsilon(\tau)\right] &= \mathscr{S}_\theta\left[{}^c\mathscr{D}^{\nu}\varepsilon(\tau)\right] = \theta^{-\nu}\varepsilon^s(\theta) - \theta^{-\nu-1}\varepsilon(0)\\
&= \theta^{-\nu}\mathscr{S}_\theta\,{}^c\mathscr{D}^{m\nu}\omega(\tau) - \theta^{-\nu-1}\,{}^c\mathscr{D}^{m\nu}\omega(\tau)\Big|_{\tau=0}\\
&= \theta^{-\nu}\left[\theta^{-m\nu}\omega^s(\theta) - \sum_{j=0}^{m-1}\theta^{(j-m)\nu-1}\,{}^c\mathscr{D}^{j\nu}\omega(\tau)\Big|_{\tau=0}\right]\\
&\quad - \theta^{-\nu-1}\,{}^c\mathscr{D}^{m\nu}\omega(\tau)\Big|_{\tau=0}\\
&= \theta^{-(m+1)\nu}\omega^s(\theta) - \sum_{j=0}^{m-1}\theta^{(j-(m+1)))\nu-1}\,{}^c\mathscr{D}^{j\nu}\omega(\tau)\Big|_{\tau=0}\\
&\quad - \theta^{\nu-1}\,{}^c\mathscr{D}^{\nu}\omega(\tau)\Big|_{\tau=0}\\
&= \theta^{-(m+1)\nu}\omega^s(\theta) - \sum_{j=0}^{m}\theta^{j-(m+1)\nu-1}\,{}^c\mathscr{D}^{j\nu}\omega(\tau)\Big|_{\tau=0}\\
&= \theta^{-k\nu}\omega^s(\theta) - \sum_{j=0}^{k-1}\theta^{(j-k)\nu-1}\,{}^c\mathscr{D}^{j\nu}\omega(\tau)\Big|_{\tau=0}.
\end{aligned} \tag{19}$$

Hence the relation (15) is true for all $k\in\mathbb{N}$. □

Recall [27] that the power series form is given by

$$\sum_{j=0}^{\infty}\omega_j(\tau)(\rho-\rho_0)^{jn} = \omega_0(\tau)(\rho-\rho_0)^0 + \omega_1(\tau)(\rho-\rho_0)^n + \omega_2(\tau)(\rho-\rho_0)^{2n} + \cdots \tag{20}$$

where $\tau = (\tau_1,\ \tau_2,\ \cdots,\ \tau_n)\in\mathbb{R}^n,\ n\in\mathbb{N}$. The Multiple Fractional Power Series (MFPS) denotes the multiple fractional power series which means the series about ρ_0 with a variable ρ and the coefficients $\omega_j(\tau)$.

Lemma 3 Let $\omega:\mathbb{J}^n\to\mathbb{R}$ be an order-exponentiation map. The MFPS notation for ω^s is given by

$$\omega^s(\theta) = \sum_{j=0}^{\infty} \frac{f_j(\tau)}{\theta^{-jn+1}} \quad \theta > 0, \tag{21}$$

where $\tau = (\tau_1,\ \tau_2,\ \cdots,\ \tau_n) \in \mathbb{R}^n$, $n \in \mathbb{N}$.

Proof. Use the Taylor series to get

$$\omega(\tau) = f_0(\tau) + f_1(\tau)\frac{\tau^n}{\Gamma(n+1)} + f_2(\tau)\frac{\tau^{2n}}{\Gamma(2n+1)} + \cdots \tag{22}$$

Take Sawi transform for (21)

$$\begin{aligned} \mathscr{S}_\theta \omega(\tau) &= \mathscr{S}_\theta f_0(\tau) + f_1(\tau)\frac{\mathscr{S}_\theta \tau^n}{\Gamma(n+1)} + f_2(\tau)\frac{\mathscr{S}_\theta \tau^{2n}}{\Gamma(2n+1)} + \cdots \\ &= \frac{f_0(\tau)}{\theta} + f_1(\tau)\frac{\Gamma(n+1)}{\theta^{-n+1}\Gamma(n+1)} + f_2(\tau)\frac{\Gamma(2n+1)}{\theta^{-2n+1}\Gamma(2n+1)} + \cdots \qquad (23) \\ &= \sum_{j=0}^{\infty} \frac{f_j(\tau)}{\theta^{-jn+1}}. \end{aligned}$$

□

Lemma 4 Let $\omega : \mathbb{J}^n \to \mathbb{R}$ be an order-exponentiation map. Then $\lim_{\theta\to 0} \theta\omega^s(\theta) = \omega(0)$ for all $\tau \in \mathbb{R}^n$.

Proof. Put $\omega(0) = f_0(\tau)$ to obtain the desired. □

Theorem 2 Let $\omega : \mathbb{J}^n \to \mathbb{R}$ be an order-exponentiation map. Then

$$\omega^s(\theta) = \sum_{j=0}^{\infty} \frac{f_j(\tau)}{\theta^{-jn+1}} \quad (0 < \nu \leq 1) \tag{24}$$

for all $\tau \in \mathbb{R}^n$ and $\theta > 0$, where $f_j(\tau) = \mathscr{D}^{jn}\omega(\tau)\Big|_{\tau=0}$.

Proof. The form of Taylor's series is given by

$$f_1(\tau) = \theta^{-n+1}\omega^s(\theta) - \theta^{-n+2}f_0(\tau) - \frac{1}{\theta^{-n}}f_2(\tau) - \frac{1}{\theta^{-2n}}f_3(\tau) - \cdots \tag{25}$$

By taking the limit of (25) when $\theta \to 0$ to obtain

$$f_1(\tau) = \lim_{\theta\to 0}\left[\theta^{-n+1}\omega^s(\theta) - \theta^{-n+2}f_0(\tau)\right]. \tag{26}$$

By Lemma 4 we have $f_1(\tau) = \mathscr{D}^n\omega(0)$. Similar, the form of Taylor's series of $f_2(\tau)$ will be

$$f_2(\tau) = \theta^{-2n+1}\omega^s(\theta) - \theta^{-2n}f_0(\tau) - \theta^{-n}f_1(\tau) - \theta^n f_3(\tau) - \cdots \tag{27}$$

Take the limit of (27) when $\theta \to 0$ to obtain

$$f_2(\tau) = \lim_{\theta \to 0} \left[\theta^{-2n+1} \omega^s(\theta) - \theta^{-2n} f_0(\tau) - \theta^{-n} f_1(\tau) \right]. \tag{28}$$

By Lemmas 2 and 4 we have $f_2(\tau) = \mathscr{D}^{2n}\omega(0)$. By the continuity, we indicate that $f_j(\tau) = \mathscr{D}^{jn}\omega(0)$. □

In theorem above we get

$$\mathscr{S}_\theta \left[{}^c\mathscr{D}^\nu \omega(\tau) \right] = \sum_{j=0}^{\infty} \frac{1}{\theta^{-j\nu+1}} {}^c\mathscr{D}^{j\nu}\omega(\tau)\Big|_{\tau=0} \qquad (0 < \nu \leq 1),$$

for all $\tau \in \mathbb{R}^n$, $\theta > 0$ and the inverse Sawi transform will be

$$\omega(\tau) = \sum_{j=0}^{\infty} \frac{{}^c\mathscr{D}^{j\nu}\omega(\tau)\Big|_{\tau=0}}{\Gamma(j\nu+1)} \quad \tau^{j\nu} \qquad (0 < \nu \leq 1),$$

for all $\tau \in \mathbb{R}^n$ and $\tau > 0$.

In the following theorem $\mathscr{R}es_n(\theta)$ denotes to the residual function of $\omega^s(\theta)$.

Theorem 3 Let $\omega : \mathbb{J}^n \to \mathbb{R}$ be an order-exponentiation map. If

$$\left|\left| \theta^r \mathscr{S}_\theta \left[{}^c\mathscr{D}^{(n+1)\nu} \omega(\tau) \right] \right|\right| \leq M,$$

for all $0 < \theta \leq q$ and $0 < \nu \leq 1$ then the residual $\mathscr{R}es_n(\theta)$ of MFPS satisfies

$$\|\mathscr{R}es_n(\theta)\| \leq \frac{M}{\theta^{-(n+1)\nu}}.$$

Proof. We use the form of Taylor's series as

$$\mathscr{R}es_n(\theta) = \omega^s(\theta) + \sum_{j=0}^{n} \frac{f_j(\tau)}{\theta^{-j\nu+1}}. \tag{29}$$

By Theorem 2 we have

$$\mathscr{R}es_n(\theta) = \omega^s(\theta) + \sum_{j=0}^{n} \frac{{}^c\mathscr{D}^{j\nu}\omega(0)}{\theta^{-j\nu+1}}. \tag{30}$$

Multiply (30) by $\theta^{-(n+1)\nu}$ to get

$$\theta^{-(n+1)\nu}\mathscr{R}es_n(\theta) = \theta^{-(n+1)\nu}\omega^s(\theta) + \sum_{j=0}^{n} \theta^{j-(n+1)\nu-1} {}^c\mathscr{D}^{j\nu}\omega(0). \tag{31}$$

By Lemma 2 we have

$$\theta^{-(n+1)\nu}\mathscr{R}es_n(\theta) = \mathscr{S}_\theta\left[{}^c\mathscr{D}^{(n+1)\nu}\omega(\tau)\right]. \tag{32}$$

Hence

$$\left|\left|\theta^{-(n+1)\nu}\mathscr{R}es_n(\theta)\right|\right| = \left|\left|\mathscr{S}_\theta\left[{}^c\mathscr{D}^{(n+1)\nu}\omega(\tau)\right]\right|\right|.$$

That is, $\left|\left|\mathscr{R}es_n(\theta)\right|\right| \leq \dfrac{M}{\theta^{-(n+1)\nu}}$. □

3. The methodology of SRPST

The Residual Power Series Method (RPSM) is a technique used by mathematical researchers to get analytical solutions of fractional Differential Equations (DEs). For instance, Yasmin and Almuqrin [27] employed RPSM in mathematical derivations. Liaqat et al. [28] developed this novel analytic technique to derive approximate solutions for Caputo time-fractional Partial Differential Equations (PDEs). Edalatpanah and Abdolmaleki [29] applied RPSM to derive analytical results for the Newell-Whitehead-Siegel equation, noting the method's simplicity in computing the coefficients of terms in a series solution using straightforward concepts of limits at infinity. Damag et al. [30] employed Laplace residual power series method in solving some fractional Hilfer equations. In another study, Liaqat et al. [31] employed RPSM to obtain analytical results for the Black-Scholes differential equations.

Here, we recall the steps of the RPSM by using Sawi transform for solving fractional order differential equations. Consider the Caputo fractional differential equation:

$${}^c\mathscr{D}^\nu\omega(\tau) = \mathscr{N}(\omega(\tau)) + \mathscr{M}(\omega(\tau)) \qquad \nu \in (0,\ 1], \tag{33}$$

where $\omega : \mathbb{J} \to \mathscr{B}$ is a a map, $\mathscr{N}$ denotes the part of nonlinear depending on the map $\omega(\tau)$ of variable τ while $\mathscr{M}$ denotes any map. The following conditions play a important role in determining the l behaviour of terms $\mathscr{M}$ and $\mathscr{N}$

$$\omega(0) = h_0. \tag{34}$$

Use the Sawi transform $\mathscr{S}_\theta$ of Eq. (33)

$$\mathscr{S}_\theta\left[{}^c\mathscr{D}^\nu\left[\omega(\tau)\right]\right] = \mathscr{S}_\theta\left[\mathscr{N}(\omega(\tau))\right] + \mathscr{S}_\theta\left[\mathscr{M}(\omega(\tau))\right]. \tag{35}$$

By Lemma 1, the Sawi transform $\mathscr{S}_\theta$ for the left side of Eq. (35) becomes

$$\mathscr{S}_\theta\left[{}^c\mathscr{D}^\nu\omega(\tau)\right]=\theta^{-\nu}\omega^s(\theta)-\theta^{-\nu-1}h_0. \tag{36}$$

Then from Eq. (35) and Eq. (36) we get

$$\omega^s(\theta)=\frac{1}{\theta}h_0+\frac{1}{\theta^{-\nu}}\mathscr{S}_\theta\left[\mathscr{N}(\mathscr{S}_\theta^{-1}(\omega^s(\theta)))\right]+\frac{1}{\theta^{-\nu}}\mathscr{S}_\theta\left[\mathscr{M}(\mathscr{S}_\theta^{-1}(\omega^s(\theta)))\right]. \tag{37}$$

The power series solution $\omega^s(\theta)$ for Eq. (35) is in solving the following equation:

$$\omega^s(\theta)=\frac{1}{\theta}h_0+\sum_{j=1}^{\infty}\frac{h_j}{\theta^{-j\nu+1}}. \tag{38}$$

By the initial condition in Eq. (33) and Lemma 1, we get the sequence $\langle\omega_n^s\rangle_{n\in\mathbb{N}\cup\{0\}}$ in Eq. (38) as a solving the following:

$$\omega_n^s(\theta)=\frac{1}{\theta}h_0+\sum_{j=1}^{n}\frac{h_j}{\theta^{-j\nu+1}}. \tag{39}$$

Now construct the residual map of Sawi transform, $\mathscr{S}_\theta\mathscr{R}es\ \ \omega$ for Eq. (37) as follow:

$$\mathscr{S}_\theta\mathscr{R}es\ \omega=\omega^s(\theta)-\frac{1}{\theta}h_0-\frac{1}{\theta^{-\nu}}\mathscr{S}_\theta\left[\mathscr{N}(\mathscr{S}_\theta^{-1}(\omega^s(\theta)))\right]-\frac{1}{\theta^{-\nu}}\mathscr{S}_\theta\left[\mathscr{M}(\mathscr{S}_\theta^{-1}(\omega^s(\theta)))\right], \tag{40}$$

and the n-th Sawi residual map $\mathscr{S}_\theta\mathscr{R}es_n\ \omega$ is

$$\mathscr{S}_\theta\mathscr{R}es_n\ \omega=\omega_n^s(\theta)-\frac{1}{\theta}h_0-\frac{1}{\theta^{-\nu}}\mathscr{S}_\theta\left[\mathscr{N}(\mathscr{S}_\theta^{-1}(\omega_n^s(\theta)))\right]-\frac{1}{\theta^{-\nu}}\mathscr{S}_\theta\left[\mathscr{M}(\mathscr{S}_\theta^{-1}(\omega_n^s(\theta)))\right]. \tag{41}$$

Note that $\mathscr{S}_\theta\mathscr{R}es\ \omega=0$ and

$$\lim_{n\to\infty}\mathscr{S}_\theta\mathscr{R}es_n\ \omega=\mathscr{S}_\theta\mathscr{R}es\ \omega,$$

for all $\theta>0$. If $\lim_{\theta\to0}\theta^{-n\nu+1}\mathscr{S}_\theta\mathscr{R}es\ \omega=0$ then $\lim_{\theta\to0}\theta^{n\nu+2}\mathscr{S}_\theta\mathscr{R}es_n\ \omega=0$ for all $0<\nu\leq1$ and $n=1,\ 2,\ 3,\ \cdots$. To find the terms h_n, we use the iterative technique in solving the following:

$$\lim_{\theta\to0}\theta^{-n\nu+1}\mathscr{S}_\theta\mathscr{R}es_n\ \omega=0, \tag{42}$$

for all $n=1,\ 2,\ 3,\ \cdots$. Next put the forms of the terms, h_n into Eq. (39) to get $\omega_n^s(\theta)$ of Eq. (37). Finally, take the inverse Sawi transform of $\omega_n^s(\theta)$ to get $\omega^n(\tau)$ of Eq. (33).

4. Approximate solutions

In this section, we will apply the SRPST to obtain analytical solutions for the fractional differential Equation (2) in the usual topological Banach space $\mathscr{B} = \mathbb{R}$. This equation represents the two-element Windkessel model, which describes the relationship between arterial pressure and the blood flow rate $\varphi(\tau)$ at time τ, as illustrated graphically in Figure 1b. The cardiac cycle functions as a closed-loop, pulsatile system in which the heart pumps blood throughout the systemic circulation, resembling a pulse wave, as depicted in Figure 1a [32]. Windkessel models are commonly utilized to describe the load on the heart while pumping blood through both the pulmonary and systemic arterial systems, as well as the relationship between blood pressure and blood flow in the aorta and pulmonary artery, further illustrated in Figure 1b.

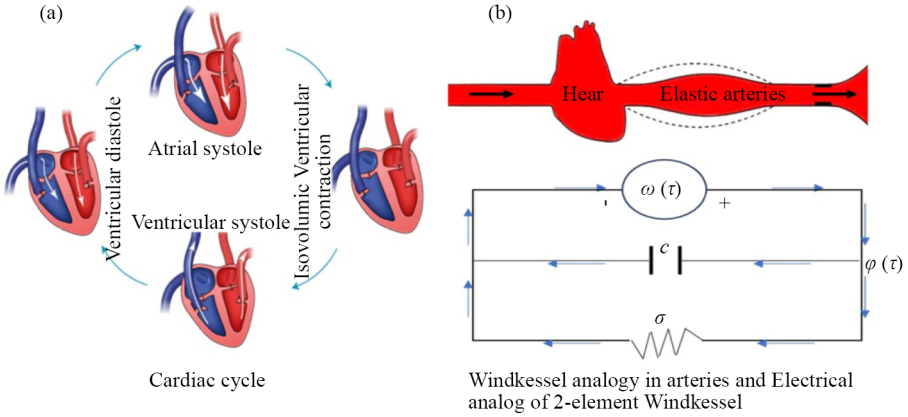

Figure 1. The human circulatory system with 2-element Windkessel model

In two-element Windkessel model, we have $\varphi(\tau) = \dfrac{\varepsilon}{\tau}$ where ε is the volume of blood being pumped at the time τ. Consider the following fractional differential equation in the usual topological Banach space $\mathscr{B} = \mathbb{R}$

$$\begin{cases} C\,{}^{c}\mathscr{D}^{\nu}\omega(\tau) + \dfrac{1}{\sigma}\omega(\tau) = \dfrac{\varepsilon}{\tau}, \quad 0 < \nu \leq 1 \\ \\ \omega(0) = C, \end{cases} \tag{43}$$

where $\omega(\tau)$ is the arterial pressure, σ is the total vascular resistance, C is the total compliance of the arterial system and ε is the volume of blood being pumped at the time τ. Here we use the SRPST to get some solutions of (43) with the initial condition $h_0 = C$. Take Sawi transforms on Eq. (43) to get

$$C \quad \mathscr{S}_\theta\left[{}^{c}\mathscr{D}^{\nu}\omega(\tau)\right] = -\frac{1}{\sigma}\mathscr{S}_\theta(\omega(\tau)) + \varepsilon\mathscr{S}_\theta\left[\frac{1}{\tau}\right].$$

Hence

$$\omega^s(\theta) = \frac{C}{\theta} - \frac{1}{\sigma C\theta^{-\nu}}\omega^s(\theta) - \frac{\varepsilon}{C\theta^{-\nu+2}}\,\mathrm{Ei}\left(-\frac{1}{\theta}\right), \tag{44}$$

with $\langle \omega_n^s \rangle_{n\in\mathbb{N}\cup\{0\}}$ as

$$\omega_n^s(\theta) = \frac{C}{\theta} + \sum_{j=1}^{n} \frac{h_j}{\theta^{-j\nu+1}}, \tag{45}$$

where Ei is an exponential Integral function has the following approximation:

$$\mathrm{Ei}(-x) = \frac{-e^{-x}}{x} \sum_{k=0}^{\infty} (-1)^k \frac{k!}{x^k}.$$

The n-th structure of Eq. (44) will be as

$$\omega_n^s(\theta) = \frac{C}{\theta} - \frac{1}{\sigma C\theta^{-\nu}} \omega_n^s(\theta) - \frac{\varepsilon}{C\theta^{-\nu+2}} \mathrm{Ei}\left(-\frac{1}{\theta}\right), \tag{46}$$

for $n = 1,\ 2,\ 3,\ \cdots$. The Sawi residual map, $\mathscr{S}_\theta \mathscr{R}es\ \omega$ for Eq. (44) as follow:

$$\mathscr{S}_\theta \mathscr{R}es\ \omega = \omega^s(\theta) - \frac{C}{\theta} + \frac{1}{\sigma C\theta^{-\nu}} \omega^s(\theta) + \frac{\varepsilon}{C\theta^{-\nu+2}} \mathrm{Ei}\left(-\frac{1}{\theta}\right), \tag{47}$$

with the n-th Sawi residual map

$$\mathscr{S}_\theta \mathscr{R}es_n\ \omega = \omega_n^s(\theta) - \frac{C}{\theta} + \frac{1}{\sigma C\theta^{-\nu}} \omega_n^s(\theta) + \frac{\varepsilon}{C\theta^{-\nu+2}} \mathrm{Ei}\left(-\frac{1}{\theta}\right), \tag{48}$$

for $n = 1,\ 2,\ 3,\ \cdots$. Now we find the terms $\langle h_n \rangle_{n\in\mathbb{N}\cup\{0\}}$ by using the following

$$\lim_{\theta\to 0} \theta^{-n\nu+1} \mathscr{S}_\theta \mathscr{R}es_n\ \omega = 0 \quad n = 1,\ 2,\ 3,\ \cdots \tag{49}$$

At $n = 1$, by using Eq. (45) we get that

$$\omega_1^s(\theta) = \frac{C}{\theta} + \frac{h_1}{\theta^{-\nu+1}},$$

and Eq. (48) becomes

$$\mathscr{S}_\theta \mathscr{R}es_1\ \omega^s(\theta) = \frac{h_1}{\theta^{-\nu+1}} + \frac{1}{\sigma\theta^{-\nu+1}} + \frac{h_1}{\sigma C\theta^{-2\nu+1}} + \frac{\varepsilon}{C\theta^{-\nu+2}} \mathrm{Ei}\left(-\frac{1}{\theta}\right). \tag{50}$$

By multiplying both sides of Eq. (50) by $\theta^{-\nu+1}$ and by using Eq. (49) we get $h_1 = \dfrac{\varepsilon\sigma - C}{C\sigma}$. At $n = 2$, by using Eq. (45) we get that

$$\omega_2^s(\theta) = \frac{C}{\theta} + \frac{h_1}{\theta^{-\nu+1}} + \frac{h_2}{\theta^{-2\nu+1}},$$

and Eq. (48) becomes

$$\mathscr{S}_\theta\mathscr{R}es_2\ \omega^s(\theta) = \frac{h_2}{\theta^{-2\nu+1}} - \frac{\varepsilon\sigma - C}{\sigma^2C^2\theta^{-2\nu+1}} - \frac{h_2}{\sigma C\theta^{-3\nu+1}} + \frac{\varepsilon}{C\theta^{-\nu+2}}\ \mathrm{Ei}\left(-\frac{1}{\theta}\right). \tag{51}$$

By multiplying both sides of Eq. (51) by $\theta^{-2\nu+1}$ and by using Eq. (49) we get $h_2 = \dfrac{\varepsilon\sigma - C}{\sigma^2C^2}$. At $n = 3$, by using Eq. (45) we have

$$\mathscr{S}_\theta\mathscr{R}es_3\ \omega^s(\theta) = \frac{h_3}{\theta^{-3\nu+1}} - \frac{\varepsilon\sigma - C}{\sigma^3C^3\theta^{-3\nu+1}} - \frac{h_3}{\sigma C\theta^{-4\nu+1}} + \frac{\varepsilon}{C\theta^{-\nu+2}}\ \mathrm{Ei}\left(-\frac{1}{\theta}\right). \tag{52}$$

By multiplying both sides of Eq. (52) by $\theta^{-3\nu+1}$ and by using Eq. (49) we get $h_3 = \dfrac{\varepsilon\sigma - C}{\sigma^3C^3}$. Hence we get that

$$h_n = \frac{\varepsilon\sigma - C}{\sigma^nC^n} \quad \text{for all} \quad n \in \mathbb{N}\cup\{0\}.$$

Put the terms of $\langle h_n\rangle_{n\in\mathbb{N}\cup\{0\}}$ in Eq. (38) to get

$$\omega^s(\theta) = C + \sum_{j=1}^{\infty} \frac{\varepsilon\sigma - C}{\sigma^jC^j\theta^{-j\nu+1}}. \tag{53}$$

Take the inverse Sawi transform of Eq. (53), to get the analytical solutions of Eq. (43)

$$\omega(\tau) = C + \sum_{j=1}^{\infty} \frac{(\varepsilon\sigma - C)\tau^{j\nu}}{\sigma^jC^j\Gamma(j\nu+1)}. \tag{54}$$

5. Numerical discussion

In this section we present some approximate solutions of Caputo fractional Windkessel model (43) with the volume of blood being pumped $\varepsilon = 60$ mL, the total vascular resistance $\sigma = 1$ and the total compliance of the arterial system $C = 1.2,\ 1.4,\ 1.6,\ 1.8$ mL/mmHg.

Tables 1 and 2 use SRPST to present some numerical solutions of Caputo fractional Windkessel model (43) for several values ν and via numerical imitation, the numerical solutions of (54) for 3th order. Figures 2 and 3 demonstrate the dynamical behaviour of some solutions of Caputo fractional Windkessel model (43). Table 1 presents some numerical solutions of Caputo fractional Windkessel model (43) at $C = 1.20,\ 1.40$, $\sigma = 22$ and several values of τ and ν. And Table 2 presents some numerical solutions of (43) at $C = 1.60,\ 1.80$.

Table 1. Some SRPST numerical solutions of (43) at $\sigma = 1$, $C = 1.20$, $C = 1.40$, $\varepsilon = 60$ with several values of ν and τ

C	τ	$\nu = 0.25$	$\nu = 0.50$	$\nu = 0.75$	$\nu = 1.00$
1.20	1.20	150.703806	144.416570	122.823750	99.2000000
	1.40	162.173640	157.043157	136.679399	113.867000
	1.60	172.889034	169.905045	149.847122	126.880000
	1.80	182.985014	182.111111	162.311598	139.320000
	2.00	192.592000	193.867778	174.180000	151.200000
	2.20	201.732805	205.178222	185.525000	162.600000
	2.40	210.425404	216.068889	196.362500	173.520000
	2.60	218.685942	226.555556	206.701389	183.960000
	2.80	226.528927	236.652222	216.537222	193.920000
	3.00	233.967136	246.361111	225.871000	203.400000
1.40	1.20	131.933160	126.755371	107.828510	86.7428570
	1.40	144.203922	140.361638	123.369580	102.257143
	1.60	156.693522	154.987498	137.830000	115.314286
	1.80	168.531271	168.041113	151.210000	127.028571
	2.00	179.774285	181.467111	163.600000	137.542857
	2.20	190.446963	194.316444	175.080000	147.028571
	2.40	200.574742	206.639722	185.740000	155.657143
	2.60	210.171639	218.441111	195.660000	163.514286
	2.80	219.251331	229.755556	204.920000	170.742857
	3.00	227.825123	240.680000	213.600000	177.400000

Table 2. Some SRPST numerical solutions of (43) at $\sigma = 1$, $C = 1.60$, $C = 1.80$, $\varepsilon = 60$ with several values of ν and τ

C	τ	$\nu = 0.25$	$\nu = 0.50$	$\nu = 0.75$	$\nu = 1.00$
1.60	1.20	116.904201	111.874953	95.1510000	75.9500000
	1.40	128.975788	126.150942	111.742500	91.8000000
	1.60	142.207236	141.818750	126.847122	105.600000
	1.80	155.719676	155.478126	140.564598	118.200000
	2.00	168.880000	170.358750	153.000000	129.600000
	2.20	181.732500	184.682500	164.262500	139.800000
	2.40	194.306000	198.358750	164.262500	148.800000
	2.60	206.629000	211.502500	174.460000	156.600000
	2.80	218.726000	224.000000	183.700000	163.200000
	3.00	230.618000	236.120000	192.090000	168.600000
1.80	1.20	110.070000	102.423810	92.6280000	74.6666670
	1.40	122.565000	117.118095	108.452500	91.2000000
	1.60	135.325000	132.271429	123.576000	106.400000
	1.80	147.495000	146.440000	138.084000	120.400000
	2.00	159.150000	161.000000	152.000000	133.200000
	2.20	170.355000	174.971429	165.342500	144.800000
	2.40	181.155000	189.142857	178.142000	155.200000
	2.60	191.595000	202.500000	190.414000	164.400000
	2.80	201.720000	216.142857	202.174000	172.400000
	3.00	211.560000	229.000000	213.440000	179.200000

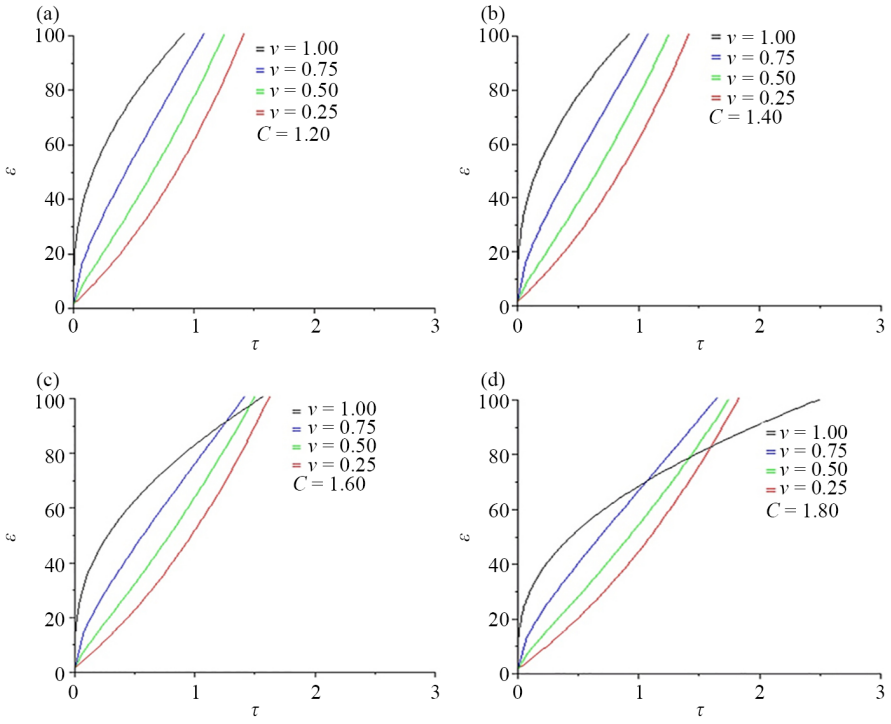

Figure 2. Some graphical SRPST solutions for (43) with $\sigma = 1$, $\varepsilon = 60$ and various values of C and ν

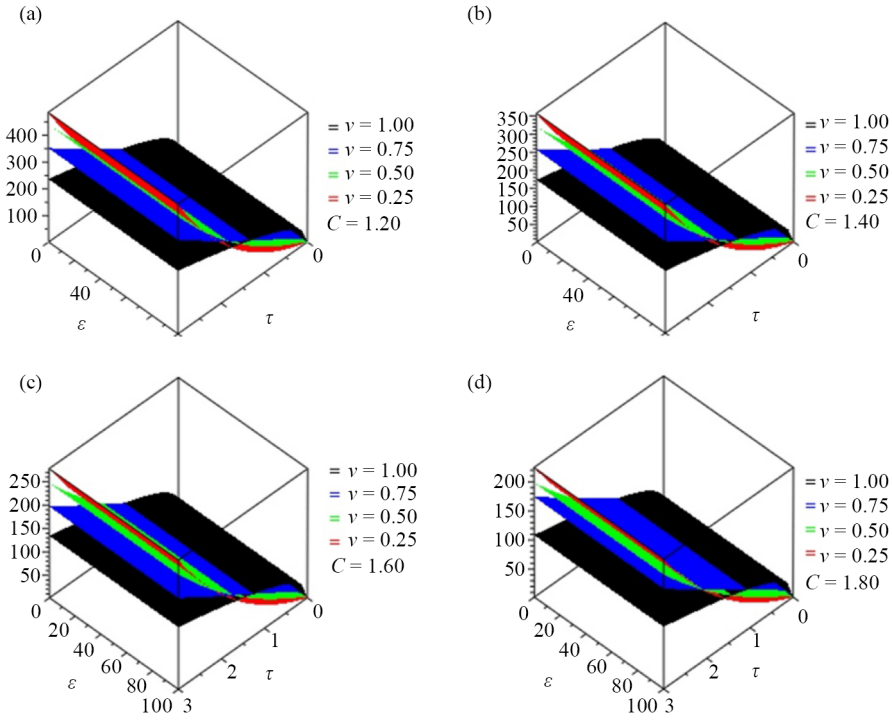

Figure 3. Some surface plots for SRPST solutions of (43) with $\sigma = 1$, $\varepsilon = 60$ and various values of C and ν

For the figures, in Figure 2, we present graphical solutions for (43) with $\nu = 0.25,\ 0.50,\ 0.75,\ 1.00$, $\sigma = 1$, $\varepsilon = 60$ and several values of C and τ. Figure 3 presents some surface plots of some analytical solutions for (43) with $\varepsilon = 60$, $\nu = 0.25,\ 0.50,\ 0.75,\ 1.00$, $C = 1.2,\ 1.4,\ 1.6,\ 1.8$ and $\sigma = 1$. The graphs and tables presented above highlight the accuracy and efficiency of the SRPST. In particular, the tables provide comparisons of the proposed method with other existing techniques across various fractional-order values, while the figures illustrate the symmetry and consistency in the graphical patterns of the three derivatives.

The findings show that SRPST yields approximate solutions that are in close agreement with both exact and numerical solutions, thereby confirming the reliability of the method. Its systematic and straightforward formulation avoids the need for linearization, discretization, or perturbation, which greatly simplifies implementation. Moreover, SRPST produces solutions in the form of rapidly convergent series, ensuring both stability and high accuracy.

A key strength of SRPST lies in its versatility, as it can be effectively applied to both linear and nonlinear fractional differential equations of varying fractional orders. From a computational perspective, it proves more efficient than many traditional numerical approaches, requiring fewer calculations to achieve comparable accuracy. In addition, the method naturally incorporates fractional derivatives and integral operators, making it well suited to contemporary fractional models. Finally, the series based structure of the solutions offers flexible control over accuracy, since additional terms can be included to refine the approximation near the exact solution, thereby balancing precision and computational cost.

6. Conclusions

The work presented above introduces the SRPST as a new method for obtaining analytical solutions to the Caputo fractional Windkessel model (43). Both the Sawi transform iterative method and SRPST have been employed to investigate this model involving the Caputo operator. This technique has proven to be an accurate and efficient tool for solving fractional differential equations.

The analytical solutions obtained through SRPST are represented as a convergent sequence $\langle h_n \rangle_{n=0}^{\infty}$. The SRPST enabled us to derive some solutions that yield promising results in conjunction with numerical simulations.

The analytical solutions highlighted the method's suitability for solving the Caputo fractional Windkessel model. The findings of this study demonstrate that SRPST is a valuable tool for future explorations, particularly in water wave equations. This is evident from the comprehensive analysis, efficacy, and reliability of SRPST, as presented in Table 1 and Figures 2 and 3. The approximate solutions derived highlight the technique's suitability for addressing complex systems in the cardiovascular domain and suggest potential applications in other fields, such as fluid dynamics and engineering. Overall, the study underscores the value of SRPST for future research endeavors.

Conflict of interest

The authors declare no competing financial interest.

References

[1] Saadeh R, Al-Wadi A, Qazza AM. Advancing solutions for fractional differential equations: Integrating the Sawi transform with iterative methods. *European Journal of Pure and Applied Mathematics*. 2025; 18(1): 5583. Available from: https://doi.org/10.29020/nybg.ejpam.v18i1.5583.

[2] Sene N. Theory and applications of new fractional order chaotic system under Caputo operator. *An International Journal of Optimization and Control: Theories and Applications*. 2022; 12(1): 20-38. Available from: https://doi.org/10.11121/ijocta.2022.1108.

[3] Sene N, Ndiaye A. Existence and uniqueness study for partial neutral functional fractional differential equation under Caputo derivative. *An International Journal of Optimization and Control: Theories and Applications*. 2024; 14(3): 208-219. Available from: https://doi.org/10.11121/ijocta.1464.

[4] Ahmed KK, Bilal M, Iqbal J, Yousif MA, Baleanu D, Mohammed PO. An analytical algebraic method for solving nonlinear fractional differential equations with conformable fractional derivatives. *Contemporary Mathematics*. 2025; 6(5): 5925-5954. Available from: https://doi.org/10.37256/cm.6520257471.

[5] Yousif MA, Baleanu D, Abdelwahed M, Azzo SM, Mohammed PO. Finite difference β-fractional approach for solving the time-fractional FitzHugh-Nagumo equation. *Alexandria Engineering Journal*. 2025; 125: 127-132. Available from: https://doi.org/10.1016/j.aej.2025.04.035.

[6] Damag FH. On comparing analytical and numerical solutions of time Caputo fractional Kawahara equations via some techniques. *Mathematics*. 2025; 13(18): 2995. Available from: https://doi.org/10.3390/math13182995.

[7] Shah K, Seadawy AR, Arfan M. Evaluation of one dimensional fuzzy fractional partial differential equations. *Alexandria Engineering Journal*. 2020; 59: 3347-3353. Available from: https://doi.org/10.1016/j.aej.2020.05.003.

[8] Kilic S, Celik E. Complex solutions to the higher-order nonlinear Boussinesq type wave equation transform. *Mathematical Research*. 2022; 73(4): 1793-1800. Available from: https://doi.org/10.1007/s11587-022-00698-1.

[9] Akgul A, Cordero A, Torregrosa JR. A fractional Newton method with 2α-order of convergence and its stability. *Applied Mathematics Letters*. 2019; 98: 344-351. Available from: https://doi.org/10.1016/j.aml.2019.06.028.

[10] Yazgan T, Ilhan E, Çelik E, Bulut H. On the new hyperbolic wave solutions to Wu-Zhang system models. *Optical and Quantum Electronics*. 2022; 54: 298. Available from: https://doi.org/10.1007/s11082-022-03683-y.

[11] Duronio F, Di Mascio A. Blood flow simulation of aneurysmatic and sane thoracic aorta using OpenFOAM CFD software. *Fluids*. 2023; 8: 272. Available from: https://doi.org/10.3390/fluids8100272.

[12] Kind T, Faes TJ, Lankhaar JW, Vonk-Noordegraaf A, Verhaegen M. Estimation of three-and four-element Windkessel parameters using subspace model identification. *IEEE Transactions on Biomedical Engineering*. 2010; 57(7): 1531-1538. Available from: https://doi.org/10.1109/TBME.2010.2041351.

[13] Fernandes M, Sousa LC, António CA, Pinto SI. Modeling the five-element Windkessel model with simultaneous utilization of blood viscoelastic properties for FFR achievement: A proof-of-concept study. *Mathematics*. 2023; 11(24): 4877. Available from: https://doi.org/10.3390/math11244877.

[14] Gnudi G. Analytical solution to Windkessel models using piecewise linear aortic flow waveform. *Physiological Measurement*. 2023; 44(6): 06NT01. Available from: https://doi.org/10.1088/1361-6579/acd6d4.

[15] Westerhof N, Lankhaar JW, Westerhof BE. The arterial Windkessel. *Medical and Biological Engineering and Computing*. 2009; 47(2): 131-141. Available from: https://doi.org/10.1007/s11517-008-0359-2.

[16] Gil A, Navarro R, Quintero P, Mares A. Transient performance analysis of centrifugal left ventricular assist devices coupled with Windkessel model: Large eddy simulations study on continuous and pulsatile flow operation. *Journal of Biomechanical Engineering*. 2024; 146(10): 101008. Available from: https://doi.org/10.1115/1.4065418.

[17] Choudhury AD, Banerjee R, Sinha A, Kundu S. Estimating blood pressure using Windkessel model on photoplethysmogram. In: *2014 36th Annual International Conference of the IEEE Engineering in Medicine and Biology Society*. Chicago, USA: IEEE; 2014. p.4567-4570.

[18] Resmi VL, Selvaganesan N. Study on fractional order arterial Windkessel model using optimization method. *IETE Journal of Education*. 2023; 64(2): 103-111. Available from: https://doi.org/10.1080/09747338.2023.2210093.

[19] Bahloul MA, Laleg-Kirati TM. Assessment of fractional-order arterial Windkessel as a model of aortic input impedance. *IEEE Open Journal of Engineering in Medicine and Biology*. 2020; 1: 123-132. Available from: https://doi.org/10.1109/OJEMB.2020.2988179.

[20] Gamilov T, Yanbarisov R. Fractional-order Windkessel boundary conditions in a one-dimensional blood flow model for fractional flow reserve (FFR) estimation. *Fractal and Fractional*. 2023; 7: 373. Available from: https://doi.org/10.3390/fractalfract7050373.

[21] Traver JE, Nuevo-Gallardo C, Tejado I, Fernández-Portales J, Ortega-Morán JF, Pagador JB, et al. Cardiovascular circulatory system and left carotid model: A fractional approach to disease modeling. *Fractal and Fractional*. 2022; 6: 64. Available from: https://doi.org/10.3390/fractalfract6020064.

[22] Belinskii ES, Liflyand ER, Trigub RM. The banach algebra A and its properties. *Journal of Fourier Analysis and Applications*. 1997; 3: 103-129. Available from: https://doi.org/10.1007/BF02649131.

[23] Damag FH, Saif A, Kilicman A. ϕ-Hilfer fractional Cauchy problems with almost sectorial and Lie bracket operators in Banach algebras. *Fractal and Fractional*. 2024; 8(12): 741. Available from: https://doi.org/10.3390/fractalfract8120741.

[24] Oqielat MA, Eriqat T, Ogilat O, El-Ajou A, Alhazmi SE, Al-Omari S. Laplace-residual power series method for solving time-fractional reaction-diffusion model. *Fractal and Fractional*. 2023; 7: 309. Available from: https://doi.org/10.3390/fractalfract7040309.

[25] Damag FH, Qurtam AA, Almalahi M, Aldwoah K, Adel M, Abd El-Latif AM, et al. A comparative analysis of harmonic mean, Holling type II, Beddington-DeAngelis, and Crowley-Martin incidence rates of a piecewise dengue fever dynamics model. *Fractal and Fractional*. 2025; 9: 400. Available from: https://doi.org/10.3390/fractalfract9070400.

[26] Sahoo M, Chakraverty S. Sawi transform based homotopy perturbation method for solving shallow water wave equations in fuzzy environment. *Mathematics*. 2022; 10: 2900. Available from: https://doi.org/10.3390/math10162900.

[27] Yasmin H, Almuqrin AH. Analytical study of time-fractional heat diffusion and Burger's equations using Aboodh residual power series and transform iterative methodologies. *AIMS Mathematics*. 2024; 9(6): 16721-16752. Available from: https://doi.org/10.3934/math.2024811.

[28] Liaqat MI, Etemad S, Rezapour S, Park C. A novel analytical Aboodh residual power series method for solving linear and nonlinear time-fractional partial differential equations with variable coefficients. *AIMS Mathematics*. 2022; 7(9): 16917-16948. Available from: https://doi.org/10.3934/math.2022929.

[29] Edalatpanah SA, Abdolmaleki E. An innovative analytical method utilizing Aboodh residual power series for solving the time-fractional Newell-Whitehead-Segel equation. *Computational Algorithms and Numerical Dimensions*. 2024; 3(2): 115-131. Available from: https://doi.org/10.22105/cand.2024.473165.1101.

[30] Damag FH, Saif A. On solving modified time Caputo fractional Kawahara equations in the framework of Hilbert algebras using the Laplace residual power series method. *Fractal and Fractional*. 2025; 9: 301. Available from: https://doi.org/10.3390/fractalfract9050301.

[31] Liaqat MI, Akgül A, Abu-Zinadah H. Analytical investigation of some time-fractional Black-Scholes models by the Aboodh residual power series method. *Mathematics*. 2023; 11: 276. Available from: https://doi.org/10.3390/math11020276.

[32] Catanho M, Sinha M, Vijayan V. *Model of Aortic Blood Flow Using the Windkessel Effect*. San Diego, USA: University of California San Diego; 2012.